# OPTICAL RECEIVER FOR SIGNALS TRANSMITTED ON FREQUENCY-MODULATED LASER CARRIERS

**Marian PEARSICĂ, Laurian GHERMAN**

"Henri Coanda" Air Force Academy, Brasov, Romania (marian.pearsica@afahc.ro, laurian.gherman@afahc.ro)

DOI: 10.19062/2247-3173.2025.26.11

***Abstract:*** *The development of wireless optical communication systems, along with the increasing application of laser technologies in space systems, has led to a growing interest in unguided optical communication, including within military domains. This paper presents the design and simulation of an optical receiver capable of demodulating unguided laser signals and reconstructing the original transmitted data. The first part of the paper outlines the architecture and key components of the optical receiver, intended for signals transmitted via an optical carrier modulated in frequency or position. Design principles, component selection, and system-level considerations are discussed in detail. In the second part, the receiver's performance is evaluated through time-domain SPICE simulations. The results confirm the correct operation of the proposed circuits and provide a basis for optimizing the receiver's performance within a wireless optical communication system. The associated optical transmitter, employing a frequency-modulated laser source, was described in a previous study and complements the system presented herein.[8].*

***Keywords:*** *optical receiver, laser carrier, wireless optical communication system*

## 1. INTRODUCTION

The proposed wireless optical communication system consists of two main subsystems: a laser transmitter [8], employing frequency or position-modulated (FM or PM) subcarriers, and an optical receiver that demodulates the unguided laser signal and reconstructs the original audio signal.

A fundamental requirement for such a system is that it offers advantages over traditional radio frequency (RF) or microwave communication systems, both in terms of performance and cost-efficiency. Free-space optical (FSO) communication [1, 2, 4] has emerged in response to the growing demand for higher data transmission rates and enhanced security. Optical links are particularly relevant in scenarios involving satellites, deep-space probes, ground stations, unmanned aerial vehicles (UAVs), high-altitude platforms, aircraft, and other communication nodes. These links are applicable in both military and civilian domains.

Free-space optical communication represents a significant step forward in the evolution of network connectivity, offering superior bandwidth, broader spectrum availability, and improved data security, thus making it a strong complement − or even an alternative to RF − based systems.

However, optical communication systems based on laser carriers are subject to various noise sources, including the quantum nature of light, shot noise in photodetectors, and disturbances introduced by the transmission medium.

In atmospheric propagation, the most significant impairments are signal fluctuation (scintillation) and attenuation of optical power.

The structure of a laser communication system is closely related to the optical demodulation technique employed. The main demodulation methods involve detecting variations in intensity, amplitude, phase, polarization, or frequency of the optical carrier. These can be implemented through direct detection, homodyne detection, frequency conversion techniques, or parameter-conversion demodulation methods.

Depending on the intended application, wireless optical communication systems can be implemented at various scales: short-range indoor systems (10–30 m), outdoor terrestrial systems (1–20 km), and long-range deep-space systems exceeding 10610^6106 km [3, 4, 6, 7].

## 2. PRINCIPLE OF OPERATION

The optical receiver is responsible for converting the incident optical signal into an electrical signal and for extracting and amplifying the information modulated onto the optical carrier [2, 3]. The photodetector performs the initial photoelectric conversion, generating a current proportional to the incident optical power, which is subsequently amplified and converted into a voltage signal.

Laser pulse detection is achieved using a photodiode matched to the emission wavelength of the laser diode (LSRD650-A5) [8]. For this purpose, the BPW20RW photodiode was selected, due to its high relative spectral sensitivity at the specific wavelength emitted by the laser source.

The optical signal, modulated at 100 kHz, is detected by the photodiode and converted into an electrical signal, which is then fed into a band-pass amplifier. This amplifier is designed to pass signals within the 70–130 kHz range, centered around the 100 kHz carrier frequency, corresponding to the sinusoidal modulating signal band of 20 Hz to 16 kHz.

The amplified signal is then buffered by a voltage follower (CI1), implemented with an operational amplifier, to provide impedance matching. This ensures the subsequent discrimination circuit is driven by a near-ideal voltage source.

The discrimination stage uses a monostable multivibrator (CI2) that generates fixed-duration output pulses corresponding to the incoming signal transitions. These pulses are then processed by a low-pass filter (CI3), implemented using an active filter (FTJ) with a cutoff frequency of approximately 16 kHz, suitable for audio signal recovery.

To correct for frequency-dependent gain introduced by the audio amplification stage in the transmitter [8], the system incorporates an integration circuit (CI4) that introduces a frequency attenuation slope of –20 dB/decade. The resulting audio signal is then amplified using a dedicated audio power amplifier (CI5), with a variable gain factor ranging from 20 to 200, effectively restoring the original analog signal from the frequency-modulated input.

For systems transmitting analog signals via pulse-modulated laser carriers, signal reconstruction is performed by low-pass filtering the sampled signal [3, 5]. The reconstruction filter (FTJ) is designed with a cutoff frequency equal to the highest frequency component of the original signal. A higher sampling rate facilitates easier filtering, as the spectral replicas of the original signal x(t)x(t)x(t) remain well separated. Conversely, a lower sampling rate increases the risk of aliasing, leading to signal distortion.

The wiring diagram of the low-pass filter is shown in Fig. 1, where (Fig. 2): $Z_3 = \frac{1}{sC_8}$;

$Z_5 = \frac{1}{sC_{10}}$; $Z_8 = \frac{1}{sC_7}$; $Z_1 = R_{11}$; $Z_2 = R_{10}$; $Z_4 = R_{12}$; $Z_6 = R_9$; $Z_7 = R_8$; $s = j\omega$.

The transfer function of the low-pass filter is of the type:

$$\frac{V_2}{V_1} = H_{TJ}(s) = \frac{a_0}{b_s s^3 + b_2 s^2 + b_1 s + b_0} \tag{1}$$

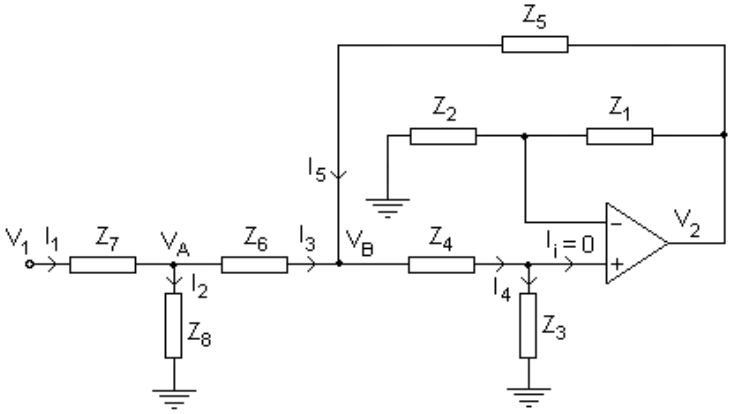


**FIG. 1** Low-Pass Filter Wiring Diagram (FTJ)

The equations underlying the determination of the transfer function of FTJ are the following (Kirchhoff's theorems apply):

$$V_+ = V_- = V_2 \frac{Z_2}{Z_1 + Z_2}\ ;\ \mathrm{I}_4 = \frac{\mathrm{V}_+}{\mathrm{Z}_3} = \mathrm{V}_2 \frac{\mathrm{Z}_2}{\mathrm{Z}_3(\mathrm{Z}_1 + \mathrm{Z}_2)};\ V_B = I_4 Z_4 + V_+ = V_2 \frac{Z_2}{Z_1 + Z_2}\left(1 + \frac{Z_4}{Z_3}\right)$$

$$I_5 = \frac{V_2 - V_B}{Z_5};\ I_3 = \frac{V_A - V_B}{Z_6} = I_4 - I_5 \tag{2}$$

Equations (2) show the following relationship between the input and output voltages of JTF:

$$V_1 = V_2\left\{\left(1 + \frac{Z_7}{Z_8} + \frac{Z_7}{Z_6}\right)\left[\frac{Z_2 Z_6}{Z_3(Z_1 + Z_2)} - \frac{Z_6}{Z_5} + \frac{Z_2}{Z_1 + Z_2}\left(1 + \frac{Z_4}{Z_3}\right)\left(1 + \frac{Z_6}{Z_5}\right)\right] - \frac{Z_7}{Z_5}\frac{Z_2}{Z_1 + Z_2}\left(1 + \frac{Z_4}{Z_3}\right)\right\} \tag{3}$$

The following expression results for the HTJ transfer function:

$$H_{TJ} = \frac{V_2}{V_1} = \frac{a_0}{\left(1 + \frac{Z_7}{Z_8} + \frac{Z_7}{Z_6}\right)\left[\frac{Z_6}{Z_3} - \frac{Z_6(Z_1 + Z_2)}{Z_5 Z_2} + \left(1 + \frac{Z_4}{Z_3}\right)\left(1 + \frac{Z_6}{Z_5}\right)\right] - \frac{Z_7}{Z_5}\left(1 + \frac{Z_4}{Z_3}\right)} \tag{4}$$

where: $a_0 = \frac{Z_1 + Z_2}{Z_2}$.

In relation (4) the eight impedances are substituted.

Taking into account the expression of the transfer function (1), for $a_0 = 2$ and $b_0 = 1$ and choosing arbitrarily $Z_1 = R_{11} = 100k\Omega$, we also get $R_{10} = R_{11} = 100k\Omega$ $R_8 << R_9$. It is considered $R_8 = 1k\Omega$, respectively, $R_9 = 10k\Omega$.

The coefficients in relation (1) will have the simplified expressions:

$$b_1 = R_8(C_7 - C_{10}) + R_9(C_8 + C_{10}) + R_{12}C_8,\ b_2 = R_8R_9C_7(C_8 - C_0) + R_{12}C_8(R_9C_{10} + R_8C_7)$$

$$b_3 = R_8R_9R_{12}C_7C_8C_{10} \tag{5}$$

The cutting frequency, $f_t = \omega_t / 2\pi$, of the filter is calculated from the relation (1), noting that at the frequency $s = j\omega = 0$, the ratio $\frac{V_2}{V_1}$ has the value $\frac{V_{20}}{V_1} = a_0 = 1 + \frac{R_{11}}{R_{10}} = 2$, and for any frequency $j\omega$ we obtain:

$$\frac{V_2}{V_{20}} = \frac{1}{b_3(j\omega)^3 + b_2(j\omega)^2 + b_1(j\omega) + 1} = \frac{1}{j\omega_t(b_1 - \omega_t^2 b_3) + 1 - \omega_t^2 b_2} \tag{6}$$

In order to obtain an attenuation of $3dB$, the following condition is met:

$$\frac{V_2}{V_{20}} = \frac{1}{\sqrt{\omega_t^2(b_1 - \omega_t^2 b_3)^2 + \left(1 - \omega_t^2 b_2\right)^2}} = \frac{1}{\sqrt{2}} \tag{7}$$

resulting in the relationship:

$$\omega_t^2(b_1 - \omega_t^2 b_3)^2 + (1 - \omega_t^2 b_2)^2 = 2 \tag{8}$$

Note that for a cut-off frequency $f_t = 16kHz$, the equation is satisfied if: $b_1 \approx 2 \cdot 10^{-5}$, $b_2 \approx 2 \cdot 10^{-10}$, respectively, $b_3 \approx 10^{-15}$. In equations (5), considering $C_{27} = 10nF$, it follows that they are satisfied for $C_8 = C_{10} = 1nF$ and $R_{12} = 10k\Omega$.

For a sinusoidal signal of constant amplitude and variable frequency, the integrating chirp provides at the output a signal with the same frequency, with amplitude dependent on frequency and circuit elements and out of phase with a phase dependent on the frequency of the signal.

The integration circuit introduces a frequency attenuation of *20dB/dec* to restore the sinusoidal signal from the line amplifier input in the electrical diagram of the laser transmitter [8] (the integrator will thus compensate for the frequency amplification achieved by the audio signal amplification circuit).

For $\underline{Z}_1 = R_{13}$ and $\underline{Z}_2 = R_{14}$ in derivation with *C13* (Fig. 2), respectively:

$$\underline{Z}_2 = \frac{R_{14}}{1 + j\omega R_{14}C_{13}} \tag{9}$$

Results:

$$A(j\omega) = -\frac{\underline{Z}_2}{\underline{Z}_1} = -\frac{R_{14}}{R_{13}(1 + j\omega R_{14}C_{13})} \tag{10}$$

Logarithm the relation (10) yields:

$$|A|_{dB} = 20\lg\frac{R_{14}}{R_{13}} - 20\lg\sqrt{1+\omega^2\tau_2^2} \tag{11}$$

where $\tau_2 = R_{14}C_{13}$. It is chosen $C_{13} = 10nF$. For an attenuation of *20dB/dec*, starting from the frequency of *20Hz*, it results:

$$f_{2i} \cong \frac{1}{2\pi\tau_2} = \frac{1}{2\pi R_{14}C_{13}} = 20Hz \quad \Rightarrow \quad R_{14} \cong 820k\Omega \tag{12}$$

## 3. SPICE ANALYSIS OF OPTICAL RECEIVER

The SPICE analysis scheme of the optical receiver is shown in Fig. 2.

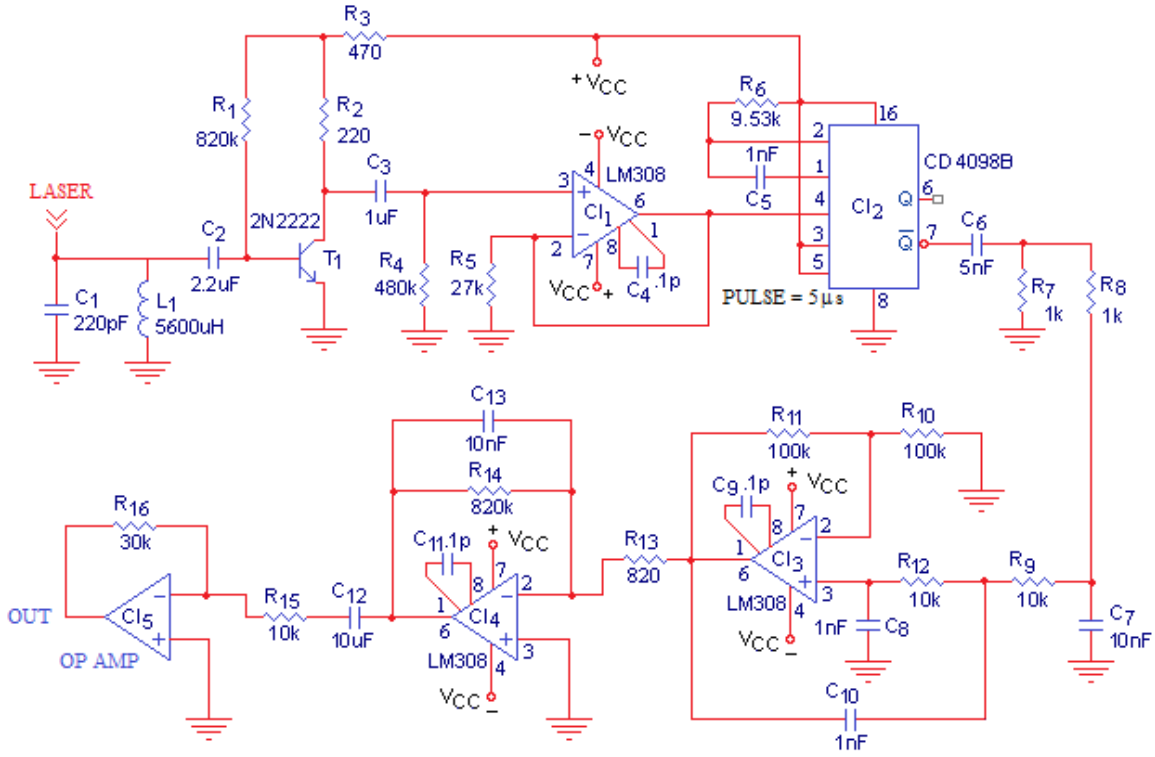


**FIG. 2** Optical Receiver SPICE Analysis Scheme

From the analysis carried out, it is observed that the cut-off frequency of the filter passes down is *16kHz*, and the integrator circuit (CI14) achieves an attenuation of the input signal by *20dB/dec*, in the frequency band *20Hz... 16kHz*. Figures 3...6 show the waveforms for: the signal at the optical receiver input (blue), the signal from the band boost output (red), the signal from the $\overline{Q}$ monostable output (green) and for the signal from the audio amplifier output (yellow), for an input signal $V_{AMPL} = 200mV$, at frequencies of *16kHz*, *10kHz*, *5kHz* and *2 kHz*.

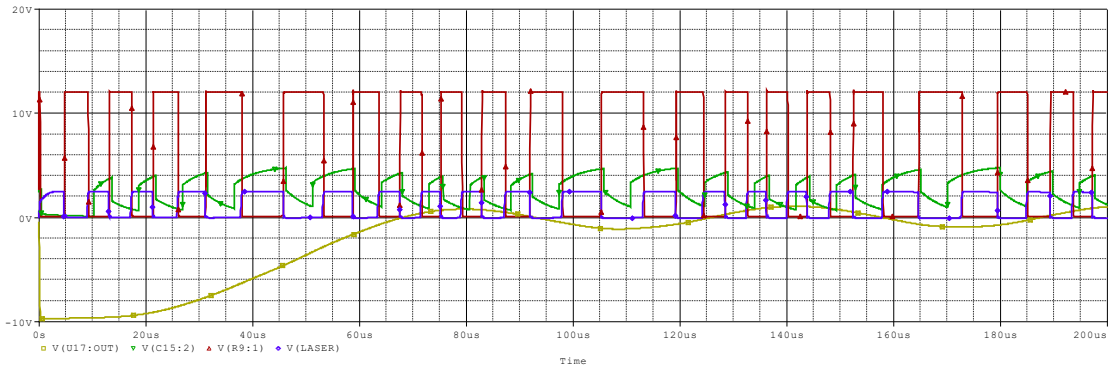


**FIG. 3** Waveforms for $V_{AMPL} = 200mV$ , $f = 16kHz$

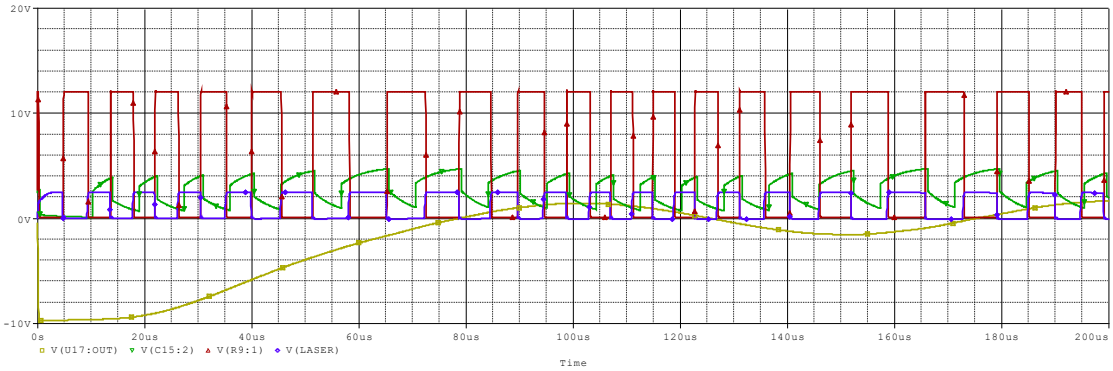


**FIG. 4** Waveforms for $V_{AMPL} = 200mV$ , $f = 10kHz$

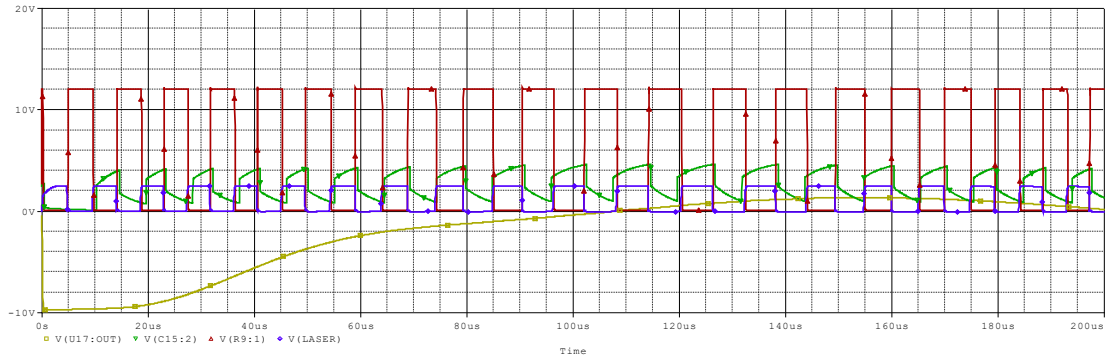


**FIG. 5** Waveforms for $V_{AMPL} = 200mV$ , $f = 5kHz$

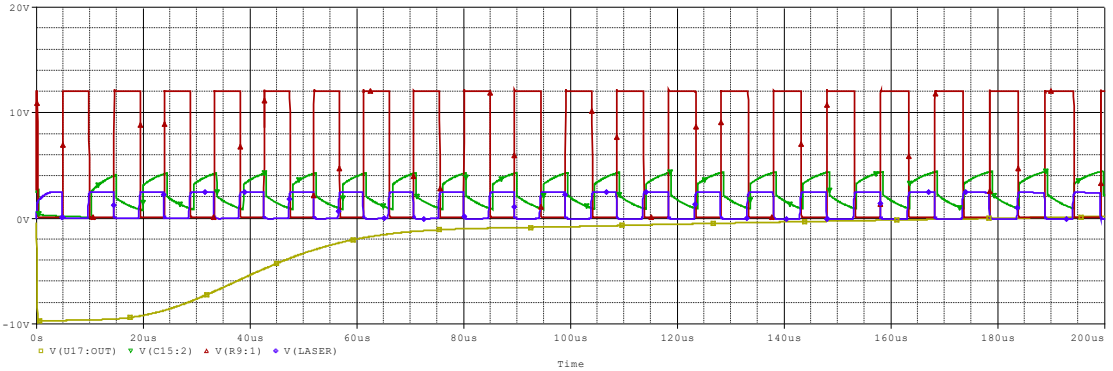


**FIG. 6** Waveforms for $V_{AMPL} = 200mV$ , $f = 2kHz$

It is observed that the signal from the output $\overline{Q}$ of the monostable has a fixed duration of $5\mu s$, the monostable being controlled on each positive front of the signal from the output of the band amplifier. The frequency of the signal obtained at the output of the monostable is variable (*70kHz... 130kHz*), depending on the frequency of the audio signal from the line amplifier input (*VAMPL).*

Figure 7 shows the comparative signals from the FTJ output (CI3) (green) and the output of the frequency attenuation circuit (CI4) (red), for a frequency of *10kHz* and an audio signal amplitude of *200mV*. Figure 8 shows the comparison of the input audio signal (*VAMPL = 200mV*) (blue) with the frequency of *10kHz* and the signal from the output of the audio amplifier (CI5) (red). It is observed that the output signal follows the input signal, having the same frequency.

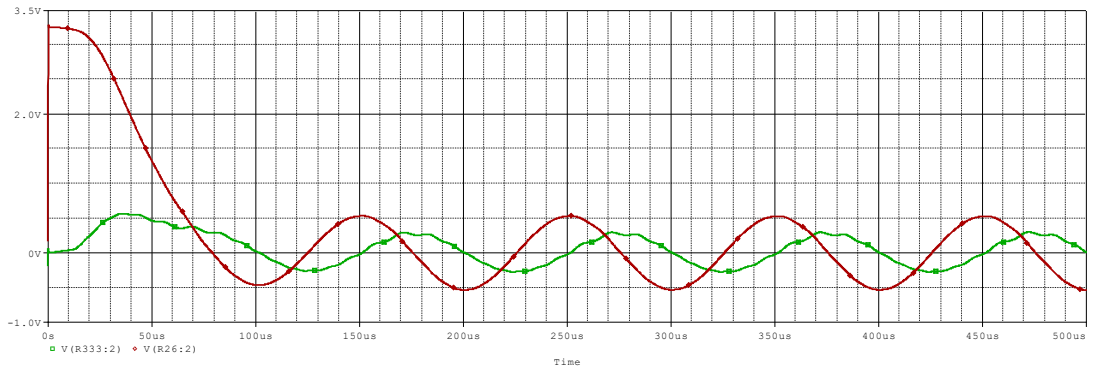


**FIG. 7** The signals at the output CI3 (FTJ) and CI4 (integrator) for $V_{AMPL} = 200mV$, $f = 10kHz$

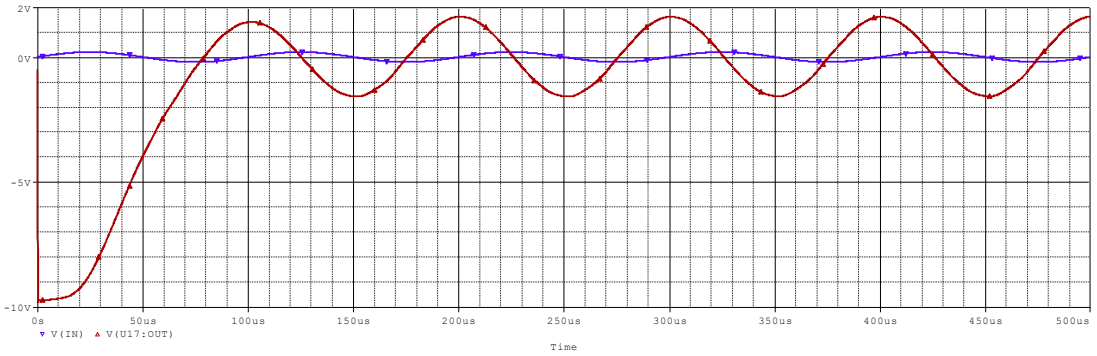


**FIG. 8** The audio signal from the input of the laser transmitter [8] and the audio signal from the output optical receiver, for $f = 10kHz$

Figures 9 and 10 show the signals from the line amplifier output (blue) and the audio amplifier output (red), for $f = 16kHz$ and $f = 5\ kHz$.

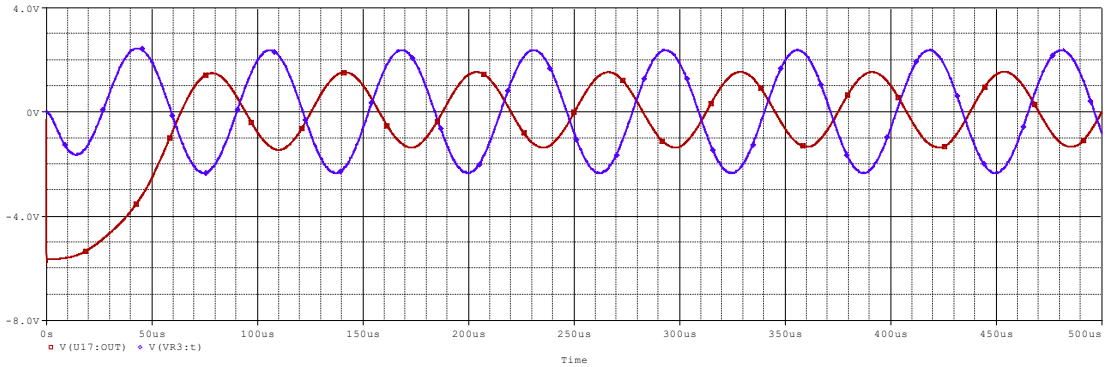


**FIG. 9** Output signals – line amplifier and audio amplifier, for $f = 16kHz$

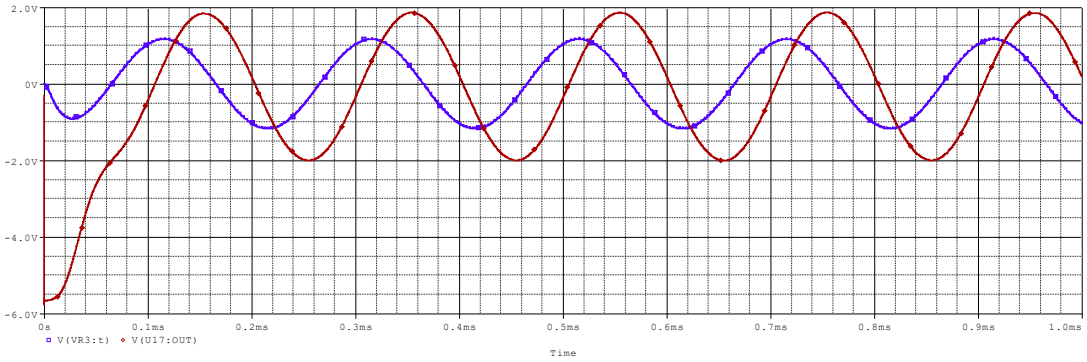


**FIG. 10** Output signals – line amplifier and audio amplifier, for $f = 5kHz$

Figure 11 shows the signals from the line amplifier output (red) and the audio amplifier output (blue) simultaneously, for two frequencies of the audio signal, $f_1 = 2kHz$ and respectively $f_2 = 20kHz$.

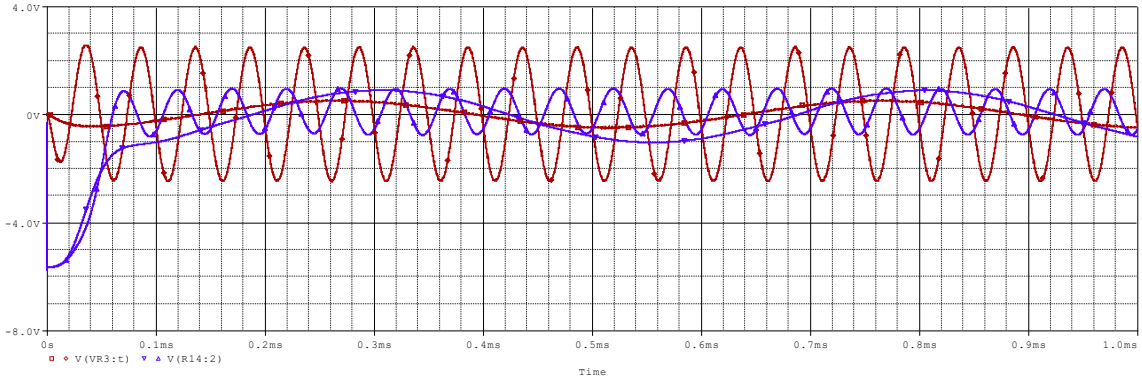


**FIG. 11** Output signals – line amplifier and audio amplifier (optical receiver)

## CONCLUSIONS

The frequency-modulated (FM) signal is demodulated using direct detection via a low-pass filter, with a cutoff frequency equal to the maximum frequency of the modulating audio signal. Since the information is conveyed through variations in frequency, the demodulation process involves converting these variations into a signal of constant amplitude. The filter effectively suppresses high-frequency components, allowing the recovery of the original baseband signal.

A key advantage of frequency modulation lies in its inherent noise immunity. As long as the amplitude of the received signal exceeds that of the noise, the detection process—based on amplitude limiting—suppresses amplitude-related noise, thereby improving the signal-to-noise ratio. The limiter ensures that the amplitude of the detected signal remains constant, further enhancing robustness against interference.

SPICE simulations confirm that the signal at the output of the audio amplifier (in the optical receiver) closely matches the frequency content of the original audio signal applied to the input of the laser transmitter [8]. The results indicate a short transient response, with the system stabilizing within a duration below $300\mu s$.

A slight time delay $35\mu s$ is observed between the input and output audio signals, which is attributed to the cumulative time constants of the analog processing circuits within both the transmitter and receiver subsystems.

## REFERENCES

[1] H. Henniger and O. Wilfert, An Introduction to Free-Space Optical Communications, *Radioengineering*, vol. 19, no. 2, pp. 203-2012, June 2010;
[2] S. Hranilovic, *Wireless Optical Communication Systems*, McMaster University, Hamilton, Springer Science Ontario, Canada, 2006;
[3] M. Carter, Laser Pointer Audio Modulator - Laser Beam Detector/Demodulator, Available: http://www.maxcarter.com; www.maxmcarter.com/lasrstuf/lasermodulator.html;
[4] A.K. Majumdar and J.C. Ricklin, *Free-Space Laser Communications. Principles and Theory*, New York (USA), Springer, 2008;
[5] L.U. Khan, *Visible light communication: Applications, architecture, standardization and research challenges*, *Digital Communication Networks*, vol. 3(2) pp. 78-88, 2016;
[6] S. Dimitrov and H. Haas, *Principles of LED Light Communications: Towards Networked Light Fidelity*, Cambridge University Press, March 2015;
[7] Z. Ghassemlooy, P. Luo and S. Zvanovec, *Optical Camera Communications*, Springer, pp 547-568, 2016;
[8] M. Pearsică and L. Gherman, Wireless Transmitter for Optical Communication with Frequency-Modulated Laser Carrier, *Review of the Air Force Academy*, No. 2 (48), pp. 53-59, 2023.